



Role of mitogen-activated protein kinases and nuclear factor-kappa B in 1,3-dichloro-2-propanol-induced hepatic injury

In-Chul Lee[#], Sang-Min Lee[#], Je-Won Ko, Sung-Hyeuk Park, In-Sik Shin,
Changjong Moon, Sung-Ho Kim, Jong-Choon Kim*

BK21 Plus Team, College of Veterinary Medicine, Chonnam National University, Gwangju 500-757, Korea

In this study, the potential hepatotoxicity of 1,3-dichloro-2-propanol and its hepatotoxic mechanisms in rats was investigated. The test chemical was administered orally to male rats at 0, 27.5, 55, and 110 mg/kg body weight. 1,3-Dichloro-2-propanol administration caused acute hepatotoxicity, as evidenced by an increase in serum aminotransferases, total cholesterol, and total bilirubin levels and a decrease in serum glucose concentration in a dose-dependent manner with corresponding histopathological changes in the hepatic tissues. The significant increase in malondialdehyde content and the significant decrease in glutathione content and antioxidant enzyme activities indicated that 1,3-dichloro-2-propanol-induced hepatic damage was mediated through oxidative stress, which caused a dose-dependent increase of hepatocellular apoptotic changes in the terminal deoxynucleotidyl transferase-mediated dUTP nick end-labeling assay and immunohistochemical analysis for caspase-3. The phosphorylation of mitogen-activated protein kinases caused by 1,3-dichloro-2-propanol possibly involved in hepatocellular apoptotic changes in rat liver. Furthermore, 1,3-dichloro-2-propanol induced an inflammatory response through activation of nuclear factor-kappa B signaling that coincided with the induction of pro-inflammatory mediators or cytokines in a dose-dependent manner. Taken together, these results demonstrate that hepatotoxicity may be related to oxidative stress-mediated activation of mitogen-activated protein kinases and nuclear factor-kappa B-mediated inflammatory response.

Keywords: 1,3-dichloro-2-propanol, hepatotoxicity, MAPKs, NF- κ B

Received 16 February 2016; Revised version received 28 February 2016; Accepted 3 March 2016

1,3-Dichloro-2-propanol (1,3-DCP) is a semivolatile organic liquid used in large volume as an intermediate for epichlorohydrin synthesis and epoxy resin production. It is also used as a precursor of 1,3-dichloropropene, a soil fumigant, and of synthetic glycerol [1]. If the chemical is released into air and wastewater, workers may be exposed to 1,3-DCP during the manufacture and use of this chemical. Exposure to 1,3-DCP may also occur from ingestion of food because it is formed when chloride ions react with lipid components under a variety of conditions, including food processing, cooking and storage [2,3].

The potential toxicity of 1,3-DCP has been investigated extensively over the past several decades using both short- and long-term animal studies [4-6]. The adverse effects associated with 1,3-DCP in humans are hepatotoxicity, irritation of mucous membranes, eyes, skin, nausea and vomiting [7]. The acute oral LD₅₀ of 1,3-DCP ranged from 110 to 400 mg/kg in rats and from 25 to 125 mg/kg in mice, depending on the purity of 1,3-DCP and the sex and strain of the rodents used [8]. Various experimental systems also demonstrated that 1,3-DCP is genotoxic, carcinogenic, neurotoxic, and embryotoxic [3,9,10]. The toxicity of 1,3-DCP to rat

[#]These authors contributed equally to this work.

*Corresponding author: Jong-Choon Kim, College of Veterinary Medicine, Chonnam National University, Gwangju 500-757, Korea
Tel: +82-62-530-2827; Fax: +82-62-530-3809; E-mail: toxkim@jnu.ac.kr

This is an Open Access article distributed under the terms of the Creative Commons Attribution Non-Commercial License (<http://creativecommons.org/licenses/by-nc/3.0>) which permits unrestricted non-commercial use, distribution, and reproduction in any medium, provided the original work is properly cited.

hepatocytes is dependent on the glutathione (GSH) status and cytochrome P450 (CYP) activity, particularly CYP2E1. The postulated CYP metabolite 1,3-dichloroacetone (1,3-DCA) is identified as being responsible for hepatocyte necrosis and other disorders [11,12]. A few publications have reported on the mechanisms of 1,3-DCP-induced hepatotoxicity. A single intraperitoneal injection of 1,3-DCP at 110 mg/kg caused an increase in malondialdehyde (MDA) level, a marker of lipid peroxidation, a decrease in glutathione *S*-transferase (GST) activity, and depletion of GSH [13]. Other mechanisms of toxic action include DNA oxidation, mitochondrial membrane potential breakdown, and intracellular calcium and reactive oxygen species (ROS) induction [14-16]. Recently, we have reported time-course changes in oxidative stress and apoptotic changes in 1,3-DCP-induced hepatotoxicity in rats [17]. However, the inflammatory effects of 1,3-DCP on liver were not evaluated in our previous study. In addition, the molecular mechanism of hepatotoxicity and dose-response effects on hepatic function are still not fully elucidated.

Therefore, the dose-related response of 1,3-DCP on hepatic function and oxidant-antioxidant balance in acute hepatic injury model is investigated. To elucidate the possible mechanism underlying its hepatotoxic effects, the histopathological and apoptotic changes with mitogen-activated protein kinases (MAPKs) in liver tissue were evaluated using immunoblotting. To evaluate the inflammatory effects of 1,3-DCP, the abundance of protein and mRNA levels of nuclear factor-kappa B (NF- κ B) and related inflammatory mediators or cytokines, including inducible nitric oxide synthase (iNOS), cyclooxygenase-2 (Cox-2), tumor necrosis factor- α (TNF- α), interleukin-1 β (IL-1 β), and IL-6 were also investigated.

Materials and Methods

Animals and environmental conditions

Specific pathogen-free male Sprague-Dawley rats aged 6 weeks (170-180 g) were obtained from Samtako Co. (Osan, Korea) and used after 1 week of quarantine and acclimation. Animals were housed in a room maintained at 23 \pm 3°C and relative humidity of 50 \pm 10% with artificial lighting from 08:00 to 20:00 and 13 to 18 air changes per hour. The rats were given sterilized tap water and commercial rodent chow (Samyang Feed, Wonju, Korea). The experimental procedure was approved

by the Institutional Animal Care and Use Committee of Chonnam National University (approve number: CNU IACUC-YB-2013-13). The animals were cared for in accordance with the Guidelines for Animal Experiments of Chonnam National University.

Test chemical and treatment

1,3-DCP (CAS No. 96-23-1; purity: 98%) was purchased from Sigma Aldrich Co. (St. Louis, MO, USA). The test chemical was dissolved in sterilized saline prepared immediately before administration. The application volume of 1,3-DCP was calculated based on the recorded body weight of the individual animal. 1,3-DCP was administered by oral gavage at a dose volume of 10 mL/kg body weight. The vehicle control rats received an equivalent volume of saline. All animals were sacrificed 12 h after 1,3-DCP administration.

Experimental groups and dose selection

Twenty-four healthy male rats were assigned randomly to four experimental groups ($n=6$): three experimental groups of 1,3-DCP receiving a single oral dose of 27.5, 55, and 110 mg/kg, respectively, and one control group. The 1,3-DCP doses were selected according to previous studies [5,17,18]. In a preliminary study, three groups of 3 male rats were exposed to 1,3-DCP at doses of 16.5, 50, and 150 mg/kg. 1,3-DCP at 150 mg/kg caused severe systemic toxicity and 2 cases of death. At 50 mg/kg, the male rats showed only an increase in serum aspartate aminotransferase (AST) level. On the basis of these results, 110 mg/kg of 1,3-DCP was selected as high dose, and 55 and 27.5 mg/kg as medium and low doses, using a scaling factor of 2 for evaluation of dose-response effects. After dose selection, three groups of 3 male rats received orally 110 mg/kg and were sacrificed at 12, 24, and 48 h. By evaluating AST levels, 12 h was chosen as an end point time after 1,3-DCP administration.

Necropsy and serum biochemical analysis

At the scheduled termination (12 h after administration), all rats were euthanized by carbon dioxide inhalation for blood collection. Blood samples were drawn from the posterior vena cava, and serum samples were collected by centrifugation at 800 \times g for 20 min within 90 min after collection. AST, alanine aminotransferase (ALT), alkaline phosphatase (ALP), total cholesterol (TCHO), total bilirubin (TBIL), triglyceride (TG), glucose (GLU), albumin (ALB), and total protein (TP) were measured

using an autoanalyzer (Dri-chem 4000i; Fujifilm Co., Tokyo, Japan).

Histopathology

A portion of the liver was dissected and fixed in 10% neutral-buffered formalin solution. The fixed liver tissues were processed routinely and were embedded in paraffin, sectioned to 4 μm thickness, deparaffinized, and rehydrated using standard techniques. 1,3-DCP-induced liver damage was evaluated by assessing morphological changes in liver sections stained with hematoxylin and eosin. All observations were made manually with a light microscope with $\times 5$, $\times 10$, $\times 20$, and $\times 40$ objective lenses and a $\times 100$ oil immersion lens in a blind manner.

Measurement of oxidative stress markers

The contents of MDA and GSH, and the activities of catalase, glutathione reductase (GR), and GST were assessed. Oxidative stress markers in liver were determined by the methods of previous studies [17,19,20]. In brief, a portion of frozen liver was homogenized in a glass-Teflon homogenizer with 50 mmol/L phosphate buffer (pH 7.4) to obtain a 1:9 (w/v) whole homogenate. The homogenates were then centrifuged at 11,000 $\times g$ for 15 min at 4°C to discard any cell debris, and the supernatant was used to measure MDA and GSH concentrations. Antioxidant enzyme activities were determined using commercial assay kits according to manufacturer's protocols (Cayman Chemical, Ann Arbor, MI, USA). Total protein contents of liver samples were determined using the method of Lowry *et al.* [21] using bovine serum albumin as standard.

Measurement of DNA fragmentation and immunohistochemical analysis for caspase-3

The fixed liver tissues were processed routinely, embedded in paraffin, sectioned to 4 μm thickness, deparaffinized, and rehydrated using standard techniques. The level of DNA fragmentation was determined using a terminal deoxynucleotidyl transferase-mediated dUTP nick end-labeling (TUNEL) assay performed according to the manufacturer's instructions (ApopTag Peroxidase *In Situ* Apoptosis Detection Kit; Chemicon, Billerica, MA, USA). The DNA fragmentation was visualized with the chromogen 3,3-diaminobenzidine (DAB). The apoptotic changes were detected using immunohistochemical analysis for caspase-3 (anti Rabbit-Specific HRP/DAB IHC Kit; Abcam, Cambridge, MA, USA)

with anti-caspase-3 antibody (1:200; Cell Signaling Technology, Beverly, MA, USA). The sections were counterstained with hematoxylin before being mounted. Each slide was examined manually with a light microscope (Leica, Wetzlar, Germany) with $\times 10$ and $\times 20$ objective lenses in a double-blind manner.

Hepatic nuclear protein isolation

Hepatic nuclear protein isolation was performed as previously. In brief, the frozen liver tissue was cut into small pieces and washed in ice-cold phosphate-buffered saline (pH 7.4). Samples were homogenized in a hypotonic lysis buffer (10 mmol/L KCl, 10 mmol/L HEPES, 0.1 mmol/L EDTA, 0.1 mmol/L EGTA) containing a protease inhibitor and dithiothreitol. Nonidet P-40 was added to a final concentration of 0.5% and the mixture was centrifuged at 250 $\times g$ for 15 min. The pellet was resuspended in extraction buffer (20 mmol/L HEPES, pH 7.9, 500 mmol/L NaCl, 1 mmol/L EDTA, 1 mmol/L EGTA, 1 mmol/L DTT) and vigorously vortexed for 15 min on ice. The nuclear suspension was centrifuged at 16,000 $\times g$ for 30 min and the supernatant was stored at -80°C for immunoblotting.

Immunoblotting

Liver tissue was homogenized (1:9, w/v) with a tissue lysis/extraction reagent (Sigma-Aldrich) containing a protease inhibitor cocktail (Sigma-Aldrich). Equal amounts of protein (40 μg /well) from each sample were separated by SDS-polyacrylamide gel electrophoresis and transferred to polyvinylidene difluoride membranes (Whatman, Maidenstone, UK). The membrane was blocked with blocking buffer (5% skim milk) for 1 h at room temperature followed by an overnight incubation at 4°C with appropriate primary antibodies. The following primary antibodies and dilutions were used: anti-Lamin B1 (1:1000 dilution; Santa Cruz Biotechnology, CA, USA), p38 MAPK, phospho-p38 MAPK (p-p38 MAPK), p44/42 MAPK (Erk1/2), p-Erk1/2, c-Jun amino-terminal kinase (JNK), p-JNK, iNOS, Cox-2, NF- κB p65, TNF- α , and β -actin (1:1000 dilution; Cell Signaling Technology, Beverly, MA, USA). The membrane was washed three times with Tris-buffered saline containing Tween 20 (TBST) and then incubated with horseradish peroxidase-conjugated secondary antibodies (1:2000 dilution; Sigma-Aldrich) for 1 h at room temperature. The blots were washed thrice with TBST and then developed using an enhanced chemiluminescence kit (Thermo

Table 1. Primer sequences for qRT-PCR

Target genes	Forward primer (5'→3')	Reverse primer (3'→5')
IL-1 β	CCC TGC AGC TGG AGA GTG TGG	TGT GCT CTG CTT GAG AGG TGC T
IL-6	CGA GCC CAC CAG GAA CGA AAG TC	CTG GCT GGA AGT CTC TTG CGG AG
iNOS	GAT TCA GTG GTC CAA CCT GCA	CGA CCT GAT GTT GCC ACT GTT
Cox-2	CCA GAG CAG AGA GAT GAA ATA CCA	GCA GGG CGG GAT ACA GTT C
TNF- α	CCA GGA GAA AGT CAG CCT CCT	TCA TAC CAG GGC TTG AGC TCA
GAPDH	AAC GGC ACA GTC AAG GCT GA	ACG CCA GTA GAC TCC ACG ACA T

IL-1 β : interleukin-1 β ; IL-6: interleukin-6; iNOS: inducible nitric oxide synthase; Cox-2: cyclooxygenase-2; TNF- α : tumor necrosis factor-alpha; and GAPDH: glyceraldehydes-3-phosphate dehydrogenase.

Scientific, Waltham, MA, USA). To determine protein expression level, each band density was quantified using TINA 20 Image software (Raytest Isotopenmessgeraete GmbH, Straubenhardt, Germany).

Quantitative real-time polymerase chain reaction (qRT-PCR)

Total RNA isolation was extracted by using TRI reagent (Molecular Research Center, Cincinnati, OH, USA) according to the manufacturer's protocol. RNA concentration was quantified using a NanoDrop ND-1000 (Thermo Scientific). Reverse transcription of an equal amount of target RNA was performed using a kit (QuantiTect Reverse Transcription, Qiagen, Valencia, CA, USA). The primer for each gene is presented in Table 1. qRT-PCR was performed using iQ SYBR Green Supermix (Bio-Rad Laboratories, Hercules, CA, USA) with a MyiQ2 thermocycler and the SYBR Green Detection System (Bio-Rad). Specific primer pairs were used to measure TNF- α , iNOS, Cox-2, IL-1 β , and IL-6 mRNA expression. The standard PCR conditions were 95°C for 15 min, 40 cycles at 95°C, 30 cycles at 60°C for 30 sec, and 72°C for 30 sec, as recommended by the primer manufacturer. The threshold cycle (C_t; the cycle number at which the amount of amplified gene of interest reached a fixed threshold) was determined subsequently. The relative values of the targets were normalized to the endogenous glyceraldehyde-3-phosphate dehydrogenase control gene and were expressed as $2^{-\Delta\Delta C_t}$ (fold), where $\Delta C_t = C_t$ of target gene - C_t of endogenous control gene and $\Delta\Delta C_t = \Delta C_t$ of samples for target gene - ΔC_t of the calibrator for the target gene.

Statistical analysis

The data are expressed as mean \pm standard deviation. Statistical significance was determined using one-way analysis of variance followed by the Dunnett's multiple

comparison tests. The data were analyzed using GraphPad InStat ver. 3.0 (GraphPad Software, Inc., La Jolla, CA, USA). A *P* value < 0.05 was considered significant.

Results

Effects of 1,3-DCP on acute hepatic damage

As shown in Table 2, serum ALP levels in the 1,3-DCP groups increased significantly in a dose-dependent manner compared with the control group. AST, ALT, TCHO, and TBIL levels also showed a significant increase, whereas GLU level exhibited a significant decrease in the 110 mg/kg group. These parameters also increased or decreased slightly in the 27.5 and 55 mg/kg groups, although statistically insignificant.

Effects of 1,3-DCP on hepatic histopathology

The results of histopathological examinations are shown in Figure 1. The control animals presented livers with normal architecture (Figure 1A). However, liver tissues from rats administered with 1,3-DCP showed various histopathological alterations, characterized by degeneration/necrosis of hepatocytes (eosinophilic cytoplasm and pyknotic changes), vacuolization, inflammatory cell infiltration, hemorrhage, and sinusoidal dilation (Figure 1B-1D). The incidence and severity of these histopathological lesions were dose-dependent.

Effects of 1,3-DCP on lipid peroxidation, GSH, and antioxidant enzyme activities

As presented in Table 3, the MDA level in the hepatic tissues increased, while GSH content decreased in the 1,3-DCP groups in a dose-dependent manner. Antioxidant enzyme activities including catalase, GR, and GST showed a dose-dependent decrease in the 1,3-DCP treated-groups.

Table 2. Serum biochemical levels of male rats treated with 1,3-DCP

Items	1,3-DCP (mg/kg)			
	0	27.5	55	110
No. of rats	6	6	6	6
AST (IU/L)	89±11 ^a	96±10	127±28	2932±283**
ALT (IU/L)	35±4	43±3	49±15	933±109**
ALP (IU/L)	130±15	177±26*	189±28**	216±38**
TCHO (mg/L)	1122±107	1160±83	1225±125	1320±180*
TBIL (mg/L)	0.40±0.05	0.45±0.06	0.47±0.05	0.90±0.17**
TG (mg/L)	265±21	275±24	358±31	150±27
GLU (mg/L)	125±13	126±13	120±14	79±15**
ALB (g/L)	3.9±0.2	4.1±0.2	3.9±0.1	4.1±0.4
TP (g/L)	5.6±0.2	5.5±0.2	5.3±0.2	5.5±0.4

1,3-DCP: 1,3-dichloro-2-propanol; AST: aspartate aminotransferase; ALT: alanine aminotransferase; ALP: alkaline phosphatase; TCHO: total cholesterol; TBIL: total bilirubin; TG: triglyceride; GLU: glucose; ALB: albumin; and TP: total protein. ^aValues are expressed as mean±SD. **P*<0.05 versus control group. ***P*<0.01 versus control group.

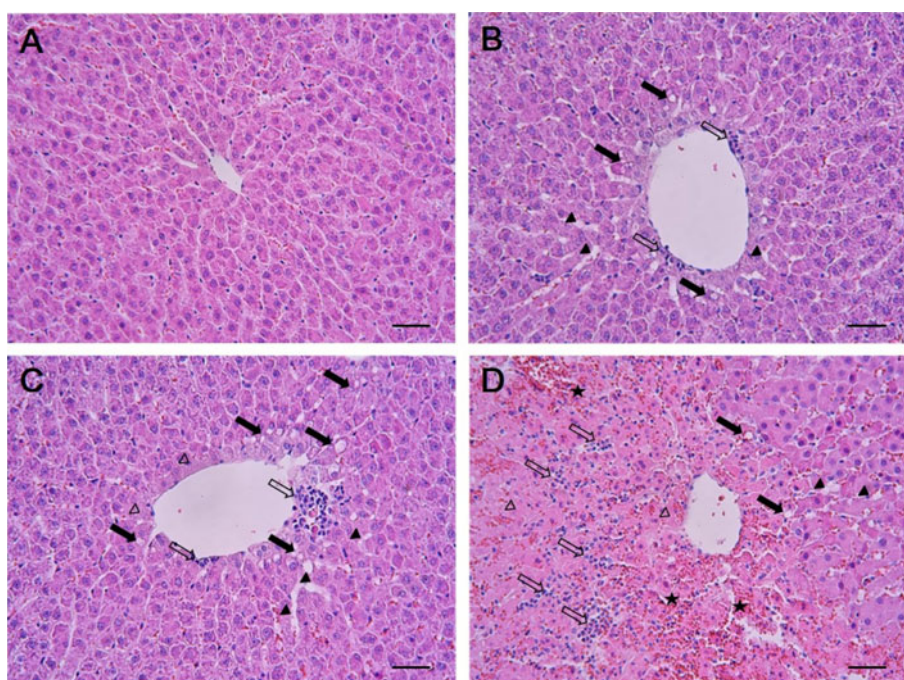


Figure 1. Effects of 1,3-DCP on hepatic histopathology. Representative photographs of liver sections of (A) control showing normal appearance and rats treated with 1,3-DCP at doses of (B) 27.5, (C) 55, and (D) 110 mg/kg showing various histopathological alterations characterized by degeneration/necrosis of hepatocytes around the central vein region (*open arrowheads*), vacuolation (*closed arrows*), inflammatory cell infiltration (*open arrows*), hemorrhage (*asterisks*), and sinusoidal dilation (*closed arrowheads*). Hematoxylin and eosin stain. Bar=50 μ m (\times 200). 1,3-DCP: 1,3-dichloro-2-propanol.

Effects of 1,3-DCP on hepatocellular apoptotic changes

As shown in Figure 2, the control and the 27.5 mg/kg groups showed few TUNEL-positive cells (Figure 2A, 2B) while there was a mild increase in the 55 mg/kg group (Figure 2C). In the 110 mg/kg group, a marked increase in the TUNEL-positive cells around the central vein was observed (Figure 2D). To further confirm the apoptotic changes caused by 1,3-DCP, an immunohistochemical analysis for caspase-3 was conducted. Caspase-

3-positive cells were seldom seen in the control and 27.5 mg/kg groups (Figure 2E, 2F). Only a few caspase-3-positive cells were observed around the centrilobular area in the 55 mg/kg group (Figure 2G), whereas caspase-3-positive cells in the 110 mg/kg group were markedly increased (Figure 2H).

Effects of 1,3-DCP on MAPKs-dependent pathways

The protein levels of phosphorylated-Erk1/2, JNK,

Table 3. Lipid peroxidation, glutathione concentration, and antioxidant enzyme activities in the liver of male rats treated with 1,3-DCP

Items	1,3-DCP (mg/kg)			
	0	27.5	55	110
No. of rats	6	6	6	6
MDA (nmol/mg protein)	0.49±0.02 ^a	0.52±0.05	0.58±0.05**	0.64±0.04**
GSH (nmol/mg protein)	3.89±0.29	3.61±0.24	3.13±0.56**	2.88±0.39**
Catalase (units/mg protein)	50±11	38±9*	35±5**	34±6.0**
GR (units/mg protein)	0.72±0.06	0.58±0.07**	0.50±0.05**	0.49±0.04**
GST (units/mg protein)	154±14	111±13**	92±18**	53±17**

^aValues are expressed as mean±SD. **P*<0.05 versus control group. ***P*<0.01 versus control group.

1,3-DCP: 1,3-dichloro-2-propanol; MDA: malondialdehyde; GSH: reduced glutathione; GR: glutathione reductase; and GST: glutathione S-transferase.

and p38 MAPK in the 1,3-DCP groups were dose-dependently increased (Figure 3A). The relative ratios of phosphorylated-MAPKs/total MAPKs also exhibited a dose-dependent increase in the 1,3-DCP-treated groups (Figure 3B-3D).

Effects of 1,3-DCP on NF-κB activation and inflammatory mediators

As shown in Figures 4 and 5, the rats receiving 1,3-DCP showed an increase in nuclear NF-κB protein levels in a dose-dependent manner (Figure 4). Similarly, hepatic TNF-α, iNOS, and Cox-2 mRNA and protein levels exhibited a dose-dependent increase (Figure 5A-5E). mRNA levels of the inflammatory cytokines IL-1β and IL-6 showed a dose-dependent up-regulation (Figure 5F and 5G).

Discussion

Previous studies have demonstrated that 1,3-DCP exposure has severe adverse effects on hepatic function and histopathology [5,7,15,18]. Although it is well known that 1,3-DCP has toxic effects on hepatic function and structure, the action mechanisms are still poorly understood. In this study, hepatocellular apoptotic changes and apoptotic cell death were mediated by oxidative stress-mediated MAPKs pathway activation are demonstrated. Changes in NF-κB-mediated inflammatory responses following 1,3-DCP treatment were also confirmed.

Injury to the hepatocytes alters membrane permeability and transport function, leading to leakage of serum aminotransferases [22,23]. The marked elevation of AST and ALT into the circulation indicates severe damage to hepatocyte membranes [5]. 1,3-DCP at 110 mg/kg caused a significant increase in serum AST and ALT levels,

indicating acute hepatotoxicity. In addition, increased ALP, TCHO, and TBIL values and decreased glucose level were observed in a dose-dependent manner. Histopathological examination confirmed the hepatotoxic effects, revealing massive hepatocellular degeneration/necrosis, inflammatory cell infiltration, hemorrhage, and sinusoidal dilation in accordance with previous studies [5,15,18]. It is well established that CYP2E1-mediated metabolism is involved in the hepatotoxicity of 1,3-DCP to yield the hepatotoxic metabolites 1,3-DCA, leading to glutathione depletion [12,14]. In addition, lipid peroxidation, DNA oxidation, intracellular Ca²⁺ increase, and generation of excessive ROS are considered to be potentially involved in 1,3-DCP-induced toxicity [13,14,16]. In this study, a single oral dose of 1,3-DCP resulted in high oxidative damage, as evidenced by a significant increase in hepatic MDA concentration and significant decreases in GSH content and GST, and catalase activities in liver tissue.

ROS-driven oxidative stress results in the activation of MAPKs that mediate cellular responses to extracellular signals. Oxidative stress caused by 1,3-DCP induced apoptotic changes in B16F10 cells, which were mediated by MAPKs, particularly phosphorylation of JNK and Erk [16]. In this study, male rats exposed to 1,3-DCP showed a dose-dependent increase in the number of TUNEL-positive cells around the centrilobular area in the hepatic tissue. To further investigate the effects of 1,3-DCP on apoptosis, immunohistochemical analysis for caspase-3 was conducted. Caspase-3 immunopositivity was also increased around the centrilobular area in a dose-dependent manner. 1,3-DCP-induced ROS initiates apoptosis via MAPKs-mediated signaling in mouse melanoma cells [16]. Thus, the expression of the MAPKs pathway-related proteins in the liver was

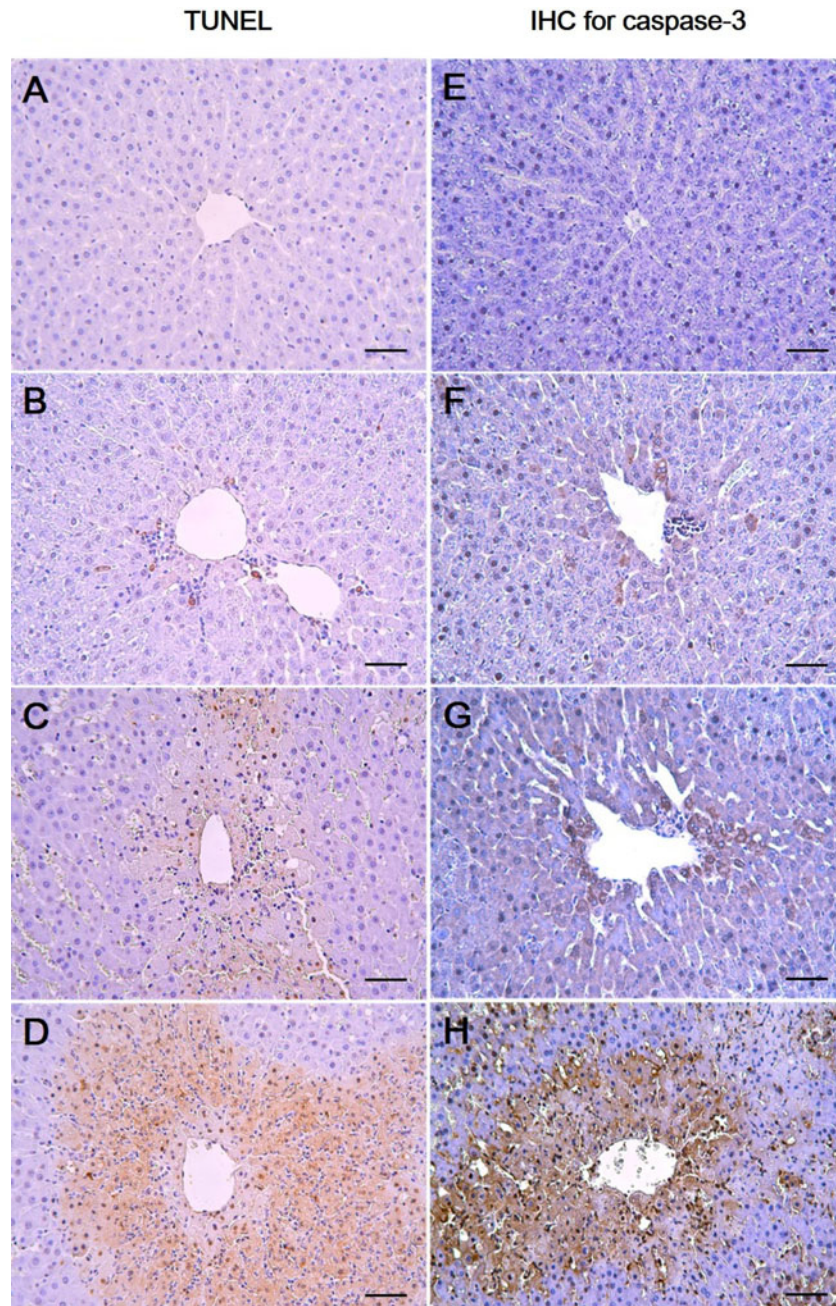


Figure 2. Effects of 1,3-DCP on hepatic cellular apoptosis. Representative photographs of TUNEL assay (A-D) and immunohistochemical analysis of caspase-3 (E-H) performed on liver sections. (A, E) Liver of control rats showed scant positive cells. The rats treated with 1,3-DCP at doses of (B, F) 27.5, (C, G) 55, and (D, H) 110 mg/kg showed a dose-dependent increase in TUNEL- and caspase-3-positive cells. Bar=50 μ m (\times 200). 1,3-DCP: 1,3-dichloro-2-propanol; and TUNEL: terminal deoxynucleotidyl transferase-mediated dUTP nick end-labeling.

investigated by immunoblotting to further understand the apoptotic cell death during 1,3-DCP intoxication. p-Erk1/2, p-JNK, and p-p38 MAPK expression levels exhibited a dose-dependent increase, well correlated with the results of the TUNEL assay and the caspase-3 immunohistochemical analysis. Therefore, oxidative

stress-mediated MAPKs signaling activation may be responsible for 1,3-DCP-induced hepatic cell apoptosis, and involved in the deterioration of liver architecture and hepatic dysfunction.

The role of NF- κ B signaling and the related inflammatory mediators have also been investigated. NF- κ B is a pivotal

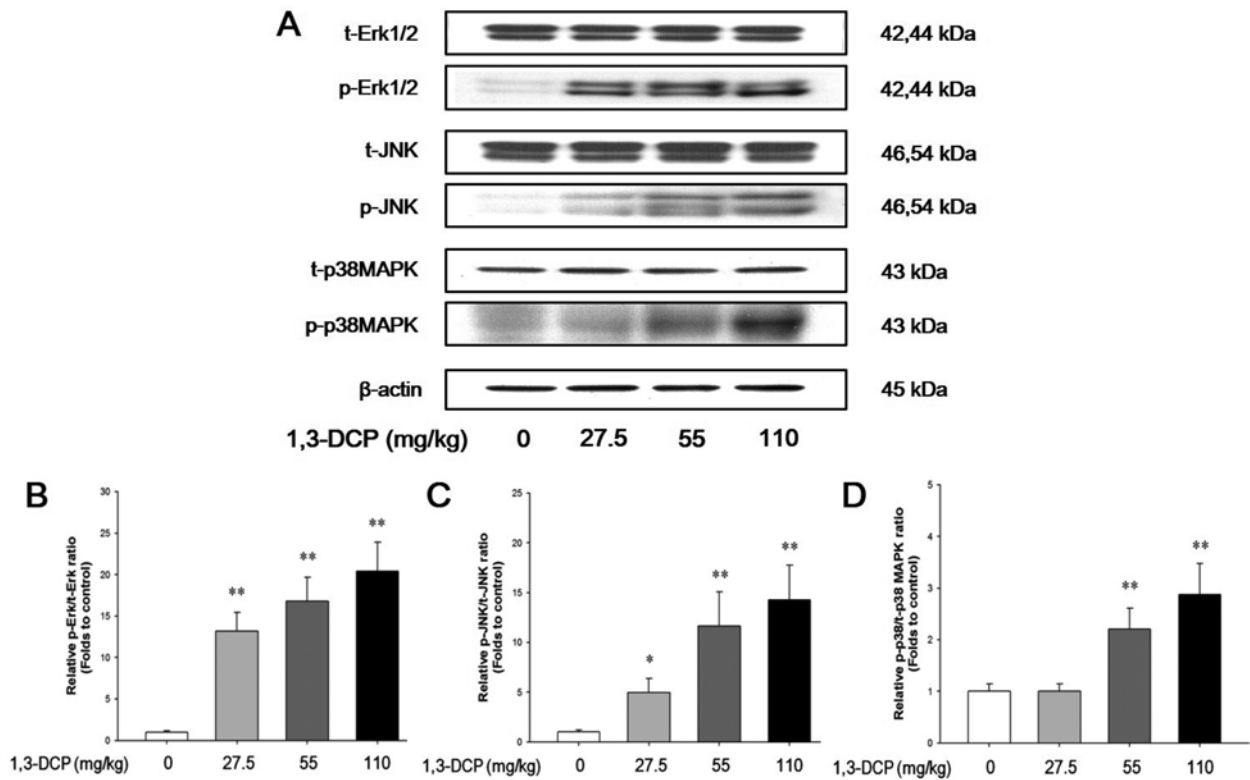


Figure 3. Effects of 1,3-DCP on MAPKs-dependent pathways. Immunoblotting analysis of (A) MAPKs-related Erk, JNK, p38 MAPK and its phosphorylated form protein levels in male rats treated with 1,3-DCP (loading control: β-actin). The bar graphs show relative (B) p-Erk/total Erk (t-Erk), (C) p-JNK/t-JNK, and (D) p-p38 MAPK/t-p38 MAPK ratios in hepatic tissues for 1,3-DCP-treated rats. Values are presented as mean±SD (n=6). *P<0.05 versus control group, **P<0.01 versus control group. 1,3-DCP: 1,3-dichloro-2-propanol; MAPKs: mitogen-activated protein kinases; Erk: p44/42 MAPK; and JNK: c-Jun N-terminal kinase.

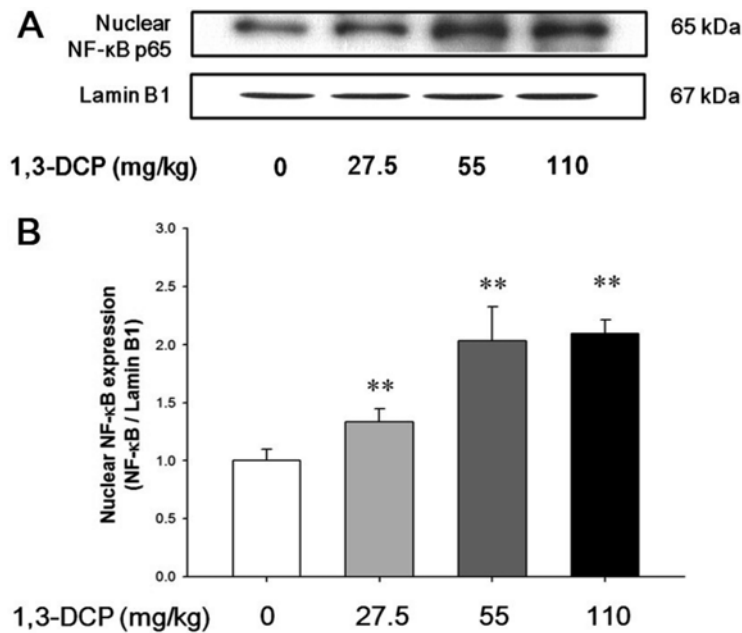


Figure 4. Effects of 1,3-DCP on NF-κB expression. (A) Immunoblotting of hepatic nuclear NF-κB expression in the male rats treated with 1,3-DCP (nuclear loading control: Lamin B1). (B) The bar graphs show relative nuclear NF-κB protein levels in hepatic tissues for 1,3-DCP treated rats. Values are presented as mean±SD (n=6). **P<0.01 versus control group. 1,3-DCP: 1,3-dichloro-2-propanol; and NF-κB: nuclear factor-kappa B.

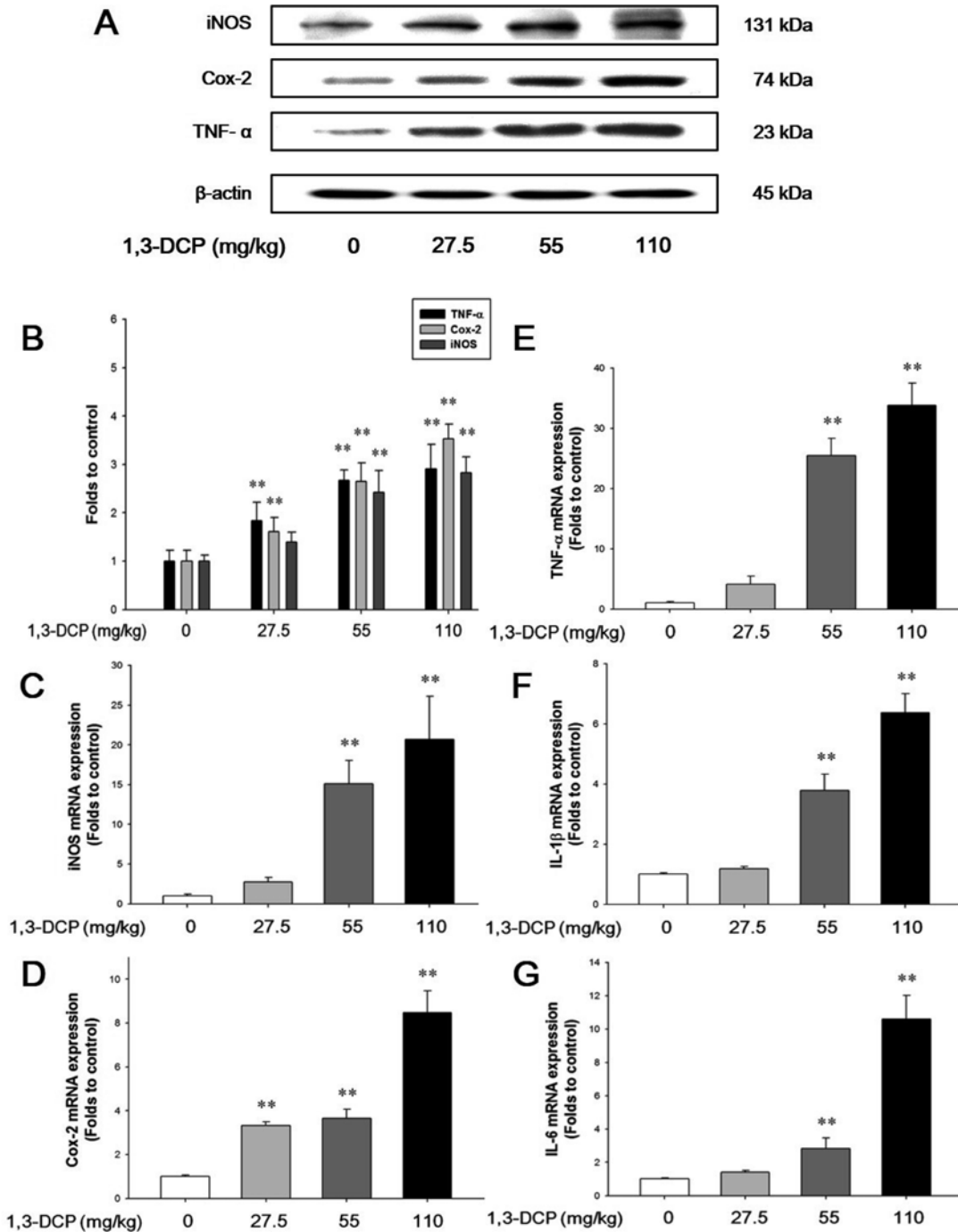


Figure 5. Effects of 1,3-DCP on NF-κB-related inflammatory mediators and cytokines. (A) Immunoblotting analysis of TNF-α, Cox-2, and iNOS expression and (B) its relative protein levels in the male rats treated with 1,3-DCP (loading control: β-actin). The bar graphs show relative mRNA levels of NF-κB-related inflammatory mediator or cytokine, (C) iNOS, (D) Cox-2, (E) TNF-α, (F) IL-1β, and (G) IL-6 mRNA levels for 1,3-DCP-treated rat (loading control: GAPDH). Values are presented as mean±SD (n=6). **P<0.01 versus control group. 1,3-DCP: 1,3-dichloro-2-propanol; NF-κB: nuclear factor-kappa B; TNF-α: tumor necrosis factor-alpha; Cox-2: cyclooxygenase-2; iNOS: inducible nitric oxide synthase; IL-1β: interleukin-1β; IL-6: interleukin-6; and GAPDH: glyceraldehydes-3-phosphate dehydrogenase.

transcription factor implicated in the regulation of inflammatory and immune responses [24]. Among various stimuli, ROS are other common signaling molecules that

induce NF-κB activation [25]. NF-κB activation and subsequent nuclear translocation induced by ROS are responsible for modulation of liver injury by affecting

cytokine production and pro-inflammatory mediators such as TNF- α , iNOS and Cox-2 [26,27]. In this study, 1,3-DCP caused nuclear translocation of NF- κ B concurrent with the induction of inflammatory mediators or cytokines including iNOS, Cox-2, TNF- α , IL-1 β , and IL-6. Therefore, hepatotoxic effects of 1,3-DCP may be attributed to inflammatory response mediated through activation of NF- κ B signaling and subsequent induction of other inflammatory mediators.

In conclusion, the results of this study suggest that 1,3-DCP elicits its hepatotoxic effects by oxidative stress, and that the effects may be related to activation of Erk1/2-, JNK-, and p38 MAPK-mediated apoptotic changes and NF- κ B signaling-mediated inflammatory responses.

Acknowledgment

This research was supported by Basic Science Research Program through the National Research Foundation of Korea funded by the Ministry of Education, Science and Technology (NRF-2013R1A1A2010835). The animal experiment in this study was supported by the Animal Medical Institute of Chonnam National University.

Conflict of interests The authors declare that there is no financial conflict of interests to publish these results.

References

1. NTP. 1,3-Dichloro-2-propanol [CAS No. 96-23-1]. Review of toxicological literature, Research Triangle Park, NC. National Toxicology Program (NTP). 2005. Available from: URL: http://ntp.niehs.nih.gov/ntp/htdocs/chem_background/exsumpdf/dichloropropanol_508.pdf. (Accessed 17 April 2015).
2. Nyman PJ, Diachenko GW, Perfetti GA. Survey of chloropropanols in soy sauces and related products. *Food Addit Contam* 2003; 20(10): 909-915.
3. Williams G, Leblanc JC, Setzer RW. Application of the margin of exposure (MoE) approach to substances in food that are genotoxic and carcinogenic: example: (CAS No. 96-23-1) 1,3-dichloro-2-propanol (DCP). *Food Chem Toxicol* 2010; 48 (S1): 57-62.
4. Jersey GC, Breslin WJ, Zeilke GJ. Subchronic toxicity of 1,3-dichloro-2-propanol in rats. *Toxicologist* 1991; 11: 353.
5. Kim HY, Lee SB, Lim KT, Kim MK, Kim JC. subchronic inhalation toxicity study of 1,3-dichloro-2-propanol in rats. *Ann Occup Hyg* 2007; 51(7): 633-643.
6. Andres S, Appel KE, Lampen A. Toxicology, occurrence and risk characterisation of the chloropropanols in food: 2-monochloro-1,3-propanediol, 1,3-dichloro-2-propanol and 2,3-dichloro-1-propanol. *Food Chem Toxicol* 2013; 58: 467-478.
7. Shiozaki T, Mizobata Y, Sugimoto H, Yoshioka T, Sugimoto T. Fulminant hepatitis following exposure to dichlorohydrin--report of two cases. *Hum Exp Toxicol* 1994; 13(4): 267-270.
8. RTECS. 1,3-Dichloro-2-propanol: toxicity, carcinogenicity, tumorigenicity, mutagenicity, and teratogenicity. Registry of Toxic Effects of Chemical Substances (RTECS) No. UB1400000. 2000. Available from: URL: <http://www.cdc.gov/niosh-rtecs/ub155cc0.html> (accessed 17 April 2015).
9. Lee JC, Shin IS, Ahn TH, Kim KH, Moon C, Kim SH, Shin DH, Park SC, Kim YB, Kim JC. Developmental toxic potential of 1,3-dichloro-2-propanol in Sprague-Dawley rats. *Regul Toxicol Pharmacol* 2009; 53(1): 63-69.
10. Lu J, Huang G, Hu S, Wang Z, Guan S. 1,3-Dichloro-2-propanol induced hyperlipidemia in C57BL/6J mice via AMPK signaling pathway. *Food Chem Toxicol* 2014; 64: 403-409.
11. Hammond AH, Garle MJ, Fry JR. Toxicity of dichloropropanols in rat hepatocyte cultures. *Environ Toxicol Pharmacol* 1996; 1(1): 39-43.
12. Hammond AH, Fry JR. Involvement of cytochrome P450E1 in the toxicity of dichloropropanol to rat hepatocyte cultures. *Toxicology* 1997; 118(2-3): 171-179.
13. Katoh T, Haratake J, Nakano S, Kikuchi M, Yoshikawa M, Arashidani K. Dose-dependent effects of dichloropropanol on liver histology and lipid peroxidation in rats. *Ind Health* 1998; 36(4): 318-323.
14. Hammond AH, Fry JR. Effect of cyanamide on toxicity and glutathione depletion in rat hepatocyte cultures: differences between two dichloropropanol isomers. *Chem Biol Interact* 1999; 122(2): 107-115.
15. Kuroda Y, Fueta Y, Kohshi K, Nakao H, Imai H, Katoh T. Toxicity of dichloropropanols. *J UOEH* 2002; 24(3): 271-280.
16. Park SY, Kim YH, Kim YH, Lee SJ. 1,3-Dichloro-2-propanol induces apoptosis via both calcium and ROS in mouse melanoma cells. *Biotechnol Lett* 2010; 32(1): 45-51.
17. Lee IC, Ko JW, Lee SM, Kim SH, Shin IS, Moon OS, Yoon WK, Kim HC, Kim JC. Time-course and molecular mechanism of hepatotoxicity induced by 1,3-dichloro-2-propanol in rats. *Environ Toxicol Pharmacol* 2015; 40(1): 191-198.
18. Haratake J, Furuta A, Iwasa T, Wakasugi C, Imazu K. Submassive hepatic necrosis induced by dichloropropanol. *Liver* 1993; 13(3): 123-129.
19. Moron MS, Depierre JW, Mannervik B. Levels of glutathione, glutathione reductase and glutathione S-transferase activities in rat lung and liver. *Biochim Biophys Acta* 1979; 582(1): 67-78.
20. Berton TR, Conti CJ, Mitchell DL, Aldaz CM, Lubet RA, Fischer SM. The effect of vitamin E acetate on ultraviolet-induced mouse skin carcinogenesis. *Mol Carcinog* 1998; 23(3): 175-184.
21. Lowry OH, Rosebrough NJ, Farr AL, Randall RJ. Protein measurement with the Folin phenol reagent. *J Biol Chem* 1951; 193(1): 265-275.
22. Kim JW, Park S, Lim CW, Lee K, Kim B. The role of air pollutants in initiating liver disease. *Toxicol Res* 2014; 30(2): 65-70.
23. Seo Y, Bazarsad D, Choe SY. Effect of acer tegmentosum maxim. Extracts on acute hepatitis and fatty liver in rats. *J Biomed Res* 2012; 13(2): 165-170.
24. Tak PP, Firestein GS. NF-kappaB: a key role in inflammatory diseases. *J Clin Invest* 2001; 107(1): 7-11.
25. Leclercq IA, Farrell GC, Sempoux C, dela Peña A, Horsmans Y. Curcumin inhibits NF-kappaB activation and reduces the severity of experimental steatohepatitis in mice. *J Hepatol* 2004; 41(6): 926-934.
26. Reyes-Gordillo K, Segovia J, Shibayama M, Vergara P, Moreno MG, Muriel P. Curcumin protects against acute liver damage in the rat by inhibiting NF-kappaB, proinflammatory cytokines production and oxidative stress. *Biochim Biophys Acta* 2007; 1770(6): 989-996.
27. Luedde T, Schwabe RF. NF- κ B in the liver--linking injury, fibrosis and hepatocellular carcinoma. *Nat Rev Gastroenterol Hepatol* 2011; 8(2): 108-118.